

Articles

Contribution from the Chemistry Division, Los Alamos National Laboratory, Los Alamos, New Mexico 87545, and the Department of Chemistry, Clemson University, Clemson, South Carolina 29634

Molecular Dynamics Studies of the Equilibrium and Saddle-Point Geometries of MX_n Molecules ($n = 2-7$)

H. K. McDowell, H.-L. Chiu, and J. F. Geldard*

Received December 4, 1987

Two nuclear potential functions that have the property of invariance to the operations of the permutation group of nuclei in molecules of the general formula MX_n , $n = 2-7$, are described. Such potential functions allow equivalent isomers to have equal energies so that various statistical mechanical properties can be simply determined. The first contains two-center interactions between pairs of peripheral atoms and is defined by $V = \frac{1}{2} \sum_{\alpha} k(\Delta r_{\alpha\mu})^2 + \sum_{\alpha < \beta} Q r_{\alpha\beta}^{-n}$ ($n = 1, 2, \dots$). The second function contains three-center interactions and is defined by $V = \frac{1}{2} \sum_{\alpha} k(\Delta r_{\alpha\mu})^2 + \frac{1}{2} \sum_{\alpha < \beta} Q r_{\alpha\beta}^{-n} (\theta_{\alpha\mu\beta} - \pi)^2$. In these equations, k and Q are force constants, $\Delta r_{\alpha\mu}$ is the change in the bond length between the X atom α and the central atom μ , and $\theta_{\alpha\mu\beta}$ is the angle subtended at the central atom by X atoms α and β for which the preferred value is π . The force fields derived from these two potential functions have been used to determine the equilibrium and saddle-point geometries of the series of molecules MX_n , $n = 2-7$. These fields predict equivalent equilibrium and saddle-point geometries for MX_2 through MX_6 but not for MX_7 . In this case, the first function gives a D_{3h} equilibrium geometry with two close-lying saddle-point geometries (the first of symmetry C_{2v} , a trigonal prism capped on a square face; the other C_{3v} , an octahedron capped on a face). The second potential function gives an equilibrium geometry with symmetry C_1 and the three geometries above as close-lying saddle-point ones. In addition, the dynamic behavior of MX_5 and MX_7 molecules follows as a natural consequence of these force fields in contrast to the relative rigidity of the others, which belong to the crystallographic point groups.

Introduction

The classical description of chemical phenomena is useful and accurate when the atoms and molecules involved are relatively heavy particles or when the temperature of the system is high; i.e., "classical mechanics emerges from quantum mechanics in the limit of large quantum numbers."¹

Various physical and chemical properties of a system can be determined by analysis of the trajectories generated by using classical molecular dynamics. The time correlation function formalism can provide important information such as the density of states in single molecules or clusters of molecules,^{2,3} the rate constants of chemical reactions⁴⁻⁷ and isomerization dynamics,⁸ and diffusion rates on crystalline metal surfaces or on metal clusters.^{9,10}

Of fundamental importance in the determination of these properties is the fact that the potential functions used in the equations of motion of the particles must reflect any symmetry properties inherent in the system. For example, in a study of the interconversion of isomers of molecules with the general formula MX_n by a nondissociative, intramolecular pathway, all equivalent isomers must have the same potential energy; i.e., the nuclear potential energy must be invariant under the operations of the permutation group of the nuclei.

The commonly used valence force fields often do not meet this requirement.¹¹⁻¹⁴ Typically, the nuclear potential energy of a molecule is defined by

$$2V = \sum_i \sum_j k_{ij} S_i S_j$$

where the k_{ij} values are force constants and the S_i values are some set of displacement coordinates. If only bond stretches and bond angle deformations need be considered, then the S_i values are defined as

$$S_i = \Delta r_{\alpha\beta} = r_{\alpha\beta} - r_{\alpha\beta}^\circ$$

for the bond stretches and

$$S_i = \Delta \theta_{\alpha\beta\gamma} = \theta_{\alpha\beta\gamma} - \theta_{\alpha\beta\gamma}^\circ$$

for the bond angle deformations, where $r_{\alpha\beta}$ and $r_{\alpha\beta}^\circ$ are the

instantaneous and equilibrium values, respectively, for the distance between atoms α and β and $\theta_{\alpha\beta\gamma}$ and $\theta_{\alpha\beta\gamma}^\circ$ are the corresponding values for the angle subtended at nucleus β by nuclei α and γ . Most molecules have more than one equilibrium value for bond lengths or bond angles. A trajectory that leads from one isomer to an equivalent one may experience a skewed potential simply because the algorithm that calculates the instantaneous forces does not recognize the need for interchange of the equilibrium reference values; i.e., the potential is not invariant to the interchange of nuclei.

In this paper, we discuss two force fields that have this property of invariance and that can be applied to MX_n molecules in which there are no nonbonding valence electrons, for example to PF_5 , SF_6 , etc. but not to TeF_4 , IF_5 , etc. The two fields are particularly appropriate to molecules in which there is substantial interaction between peripheral X atoms. We believe that these fields will prove to be useful for the simulation of molecular properties by using molecular dynamics. The first is a two-center force field derived from the static potential most recently discussed by Thompson and Bartell.¹⁵ The potential is defined by

$$V(r) = \frac{1}{2} \sum_{\alpha} k(\Delta r_{\alpha\mu})^2 + \sum_{\alpha < \beta} Q r_{\alpha\beta}^{-n} \quad (n = 1, 2, \dots) \quad (1)$$

where k and Q are force constants, $\Delta r_{\alpha\mu} = r_{\alpha\mu} - r_{\alpha\mu}^\circ$ is the change

- (1) Miller, W. H. *Science (Washington, D.C.)* **1986**, *233*, 171.
- (2) Geldard, J. F.; Pratt, L. R. *J. Chem. Educ.* **1987**, *64*, 425.
- (3) Brawer, S. *J. Chem. Phys.* **1983**, *79*, 4539.
- (4) Northrup, S. H.; Hynes, J. T. *J. Chem. Phys.* **1978**, *69*, 5246.
- (5) Northrup, S. H.; Hynes, J. T. *J. Chem. Phys.* **1980**, *73*, 2700.
- (6) Grote, R. F.; Hynes, J. T. *J. Chem. Phys.* **1981**, *74*, 4465.
- (7) Tully, J. C.; Gilmer, G. H.; Shugard, M. *J. Chem. Phys.* **1979**, *71*, 1630.
- (8) Chandler, D. *J. Chem. Phys.* **1978**, *68*, 2959.
- (9) Grimmelmann, E. K.; Tully, J. C.; Helfand, E. *J. Chem. Phys.* **1981**, *74*, 5300.
- (10) Doll, J. D.; McDowell, H. K. *J. Chem. Phys.* **1982**, *77*, 479.
- (11) Urey, H. C.; Bradley, C. A., Jr. *Phys. Rev.* **1931**, *38*, 1969.
- (12) Nakagawa, I.; Shimanouchi, T. *Spectrochim. Acta* **1962**, *18*, 89, 101.
- (13) Hiraishi, T.; Nakagawa, I.; Shimanouchi, T. *Spectrochim. Acta* **1962**, *20*, 819.
- (14) Heath, D. F.; Linnett, J. W. *Trans. Faraday Soc.* **1948**, *44*, 556, 873, 878, 884.
- (15) Thompson, H. B.; Bartell, L. S. *Inorg. Chem.* **1968**, *7*, 488.

* To whom correspondence should be addressed at Clemson University.

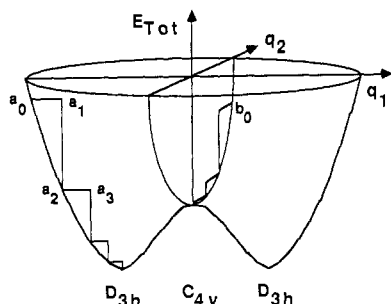


Figure 1. Total energy E_{Tot} for an MX_5 molecule as a function of the coordinates q_1 and q_2 . The coordinate q_1 leads from the one D_{3h} geometry over the barrier where at the maximum the geometry is C_{4v} down to another D_{3h} geometry. The coordinate q_2 preserves the C_{4v} symmetry of the saddle-point geometry and is orthogonal to q_1 . Similar figures apply to other MX_n molecules, as discussed in the text.

in the equilibrium bond length $r_{\alpha\mu}^\circ$ between nucleus α and the central atom μ , and $r_{\alpha\beta}$ is the distance between the X nuclei α and β .

The second potential contains a three-center interaction and is defined by

$$V(\theta) = \frac{1}{2} \sum_{\alpha} k(\Delta r_{\alpha\mu})^2 + \frac{1}{2} \sum_{\alpha < \beta} Q(r_{\alpha\beta}^\circ)^2 (\theta_{\alpha\mu\beta} - \pi)^2 \quad (2)$$

where $\theta_{\alpha\mu\beta}$ is the angle subtended by X atoms α and β at the central atom and Q is the force constant. The angle π (180°) is the angle that any two ligand nuclei would prefer to subtend at the central nucleus.

These two force fields have some important similarities and some equally important differences. Both fields will drive pairs of peripheral atoms to be diametrically opposite one another and thus to some extent would be expected to give similar geometries. On the other hand, while the angle $\theta_{\alpha\mu\beta}$ can be expressed in terms of the internuclear distance $r_{\alpha\beta}$, $V(\theta)$ can be differentiated independently with respect to both $\Delta r_{\alpha\mu}$ and $\theta_{\alpha\mu\beta}$. $V(r)$, however, cannot be differentiated independently with respect to both $\Delta r_{\alpha\mu}$ and $r_{\alpha\beta}$. Interplay between bond stretching and the optimum molecular geometry will occur, interplay that will clearly be a function of the value of the exponent n in eq 1 and that will result in as many different bond lengths as there are local symmetries in the MX_n structure. The geometries obtained by use of the function $V(\theta)$ (eq 2) will be independent of the value of $r_{\alpha\mu}^\circ$ and are thus valid for all MX_n molecules.

The two derived force fields do in fact give equivalent equilibrium and saddle-point geometries for MX_n molecules with $n = 2-6$ but do not for $n = 7$. Previous discussions of the structure of MX_n molecules have been based on static models for the potentials¹⁶⁻¹⁸ or on quantum-mechanical considerations.¹⁹⁻²¹ There are some important differences between these results and ours.

In the Computational Section, we show how the equilibrium and saddle-point geometries were determined. In the Results and Discussion, we analyze the implications of the results, especially as they relate to the chemical and physical properties of examples of MX_n molecules.

Computational Section

Hamilton's equation of motion in a Cartesian basis was solved by fourth-order Runge-Kutta integration. Trajectories begin from an initial set of positions for the $n + 1$ particles of MX_n , the only required equilibrium input being the bond lengths. Equilibrium geometries were obtained by allowing a trajectory to begin at a randomly chosen set of coordinates with zero momenta for all particles and to continue under the influence of the force field for a specified number of integration steps (usually about 20 steps with a time increment of 25 au/step) after which the momenta of the particles were reset to zero and the new trajectory

was followed. This is shown schematically in Figure 1 in which the total vibrational energy for an MX_5 molecule is plotted as a function of two displacement coordinates, q_1 and q_2 . The coordinate q_1 corresponds to the reaction coordinate that leads from the D_{3h} geometry through a C_{4v} intermediate to another D_{3h} geometry. Choose an initial geometry not in the plane E_{Tot}, q_2 ($q_1 = 0$). Since all components of momenta are set equal to zero, the total energy is equal to the potential energy and has a value a_0 . The system is then moved by the force field away from the surface and reaches the position a_1 in 20 integration steps. At a_1 , the kinetic energy is no longer zero. Resetting all components of momenta to zero again drops the total energy from a_1 away from the surface to a_2 back on the surface, and the process is repeated until the system reaches the bottom of the well. Because of the invariant nature of the two potential functions, it does not matter which well is reached. Between 2000 and 8000 integration steps usually were needed to bring the system to the equilibrium geometry, at which point the kinetic energy of the system remains zero and the particles experience no force.

Saddle-point geometries were obtained by the same method except that the initial geometry must be chosen such that the forces cause the trajectories to alight on the saddle-points. This is accomplished by choosing an initial geometry that has the same point symmetry as does the saddle-point geometry. Then there is no component of the force field in the direction of the reaction coordinate that leads from the saddle-point geometry to the equilibrium geometry. For example, the initial choice for the C_{4v} saddle-point geometry of MX_5 is a square pyramid with the M nucleus in its base. As shown in Figure 1, this might correspond to a total energy of b_0 . The force field acting on this geometry has no component in the direction q_1 , and thus during cooling, the only minimum that can be reached is the one in the E_{Tot}, q_2 ($q_1 = 0$) plane.

These processes for finding the equilibrium and saddle-point geometries are analogous to cooling or annealing trajectories with a friction constant that is determined by the number of steps between momentum resets. Any higher energy minima will not necessarily be detected by this method.

The computer code that was used to perform these calculations is written in double-precision Fortran and has been described earlier.²² The algorithm has been tested by calculating the density of states versus frequencies of vibration by Fourier transforming trajectory velocity data and then comparing the frequencies against the results of a separate normal-coordinate analysis calculation and the number of degrees of freedom with the group-theoretic result. The calculations were run on a Digital Vax 8650 machine configured with a Digital MicroVax II computer.

Results and Discussion

Although MX_2 and MX_3 molecules have only one quantum-mechanical isomer each, we begin by comparing their equilibrium geometries that are predicted by the two force fields derived from eq 1 and 2. These two force fields are given by

$$-\frac{\partial V}{\partial x_{i\sigma}} = -\sum_{\alpha} k(r_{\alpha\mu} - r_{\alpha\mu}^\circ) \frac{\partial r_{\alpha\mu}}{\partial x_{i\sigma}} + \sum_{\alpha < \beta} n Q r_{\alpha\beta}^{-n-1} \frac{\partial r_{\alpha\beta}}{\partial x_{i\sigma}} \quad (3)$$

derived from eq 1, and

$$-\frac{\partial V}{\partial x_{i\sigma}} = -\sum_{\alpha} k(r_{\alpha\mu} - r_{\alpha\mu}^\circ) \frac{\partial r_{\alpha\mu}}{\partial x_{i\sigma}} + \sum_{\alpha < \beta} (r_{\alpha\mu}^\circ)^2 Q (\theta_{\alpha\mu\beta} - \pi) \frac{\partial \theta_{\alpha\mu\beta}}{\partial x_{i\sigma}} \quad (4)$$

derived from eq 2, where $x_{i\sigma}$ is the i th Cartesian coordinate of nucleus σ . We refer to these fields as field I and field II, respectively. In eq 3, the potential energy cannot be minimized separately with respect to variation in bond length and variation in interligand distance because the second distance is an implicit function of the first. In eq 4, however, the potential energy can be minimized separately with respect to variations in bond length and bond angle. This leads to a quantitative difference in the equilibrium and saddle-point geometries determined by these two fields. In geometries generated by field II, all bond lengths equal exactly the input equilibrium bond lengths, whereas, in those of field I, interligand repulsion can be alleviated by internal energy conversion with the result that all bonds are slightly longer than the input equilibrium bond lengths, making the total energy of the system lower.

(16) Gillespie, R. J.; Nyholm, R. S. *Q. Rev., Chem. Soc.* **1957**, *11*, 339.
 (17) Gillespie, R. J. *Can. J. Chem.* **1960**, *38*, 818.
 (18) Gillespie, R. J. *J. Chem. Educ.* **1963**, *40*, 295.
 (19) Vicharelli, P. A.; McDonald, F. A. *J. Chem. Phys.* **1980**, *72*, 4627.
 (20) Rothman, M. J.; Bartell, L. S.; Ewig, C. S.; Van Wazer, J. R. *J. Chem. Phys.* **1980**, *73*, 375.
 (21) Marsden, C. J. *J. Chem. Soc., Chem. Commun.* **1984**, 401.

(22) Geldard, J. F.; McDowell, H. K. *Spectrochim. Acta, Part A* **1987**, *43A*, 439.

Table I. Energies and Bond Lengths of the Equilibrium and Saddle-Point Geometries of MX_n Molecules Using the $1/r$ Potential Function

species (sym)	bond length, ^a Å	energy, hartrees		
		Δr	$1/r$	tot.
MX_2	1.6065	0.0030	0.2022	0.2052
MX_3	1.6605	0.0205	0.6678	0.6983
$\text{MX}_4 (T_d)$	1.7107	0.0615	1.3957	1.4571
$\text{MX}_4 (D_{4h})$	1.7161	0.0659	1.4497	1.5156
$\text{MX}_5 (D_{3h})$	1.7630 (2)	0.1361	2.3897	2.5259
	1.7590 (3)			
$\text{MX}_5 (C_{4v})$	<i>b</i>	0.1365	2.3927	2.5292
$\text{MX}_5 (D_{5h})$	1.7708	0.1503	2.5255	2.6758
$\text{MX}_6 (O_h)$	1.8052	0.2441	3.5944	3.8384
$\text{MX}_6 (D_{3h})$	1.8073	0.2484	3.6299	3.8783
$\text{MX}_6 (C_{3v})$	1.7982 (1)	0.2544	3.6793	3.9338
	1.8127 (5)			
$\text{MX}_6 (D_{6h})$	1.8238	0.2825	3.9065	4.1890
$\text{MX}_7 (D_{5h})$	1.8433 (2)	0.3977	5.0772	5.4749
	1.8523 (5)			
$\text{MX}_7 (C_{3v}[1,3,3]s)$	<i>b</i>	0.3979	5.0791	5.4770
$\text{MX}_7 (C_{2v}[1,4,2])$	<i>b</i>	0.3979	5.0789	5.4767
$\text{MX}_7 (C_{2v}[1,2,4])$	<i>b</i>	0.4079	5.1526	5.5605
$\text{MX}_7 (C_{3v}[1,3,3]e)$	<i>b</i>	0.4081	5.1542	5.5623
$\text{MX}_7 (C_{6v})$	1.8360 (1)	0.4229	5.2595	5.6824
	1.8624 (6)			
$\text{MX}_7 (D_{7h})$	1.8748	0.4695	5.5918	6.0613

^aThe number of bonds of a given length is shown in parentheses.^bStructural details shown in Figure 1.

Moreover, in those systems having two or more different kinds of bonds because of symmetry considerations, field I generates two or more different bond lengths, while field II always generates the one bond length. We refer to the energy associated with the first term on the right hand side of eq 1 as the Δr energy and to that associated with the second term as the $1/r$ energy. These two energies are shown with the total potential energy in Table I. In the analysis that follows, we use the values $k = 5.90$ mdyne/Å, $Q = 1.228$ (units of mdyne Å^{*n*+1} or mdyne/Å for eq 1 and 2, respectively),²² and $r_0 = 1.56$ Å for the input equilibrium bond length in all MX_n .²³ The values of k and of Q are those calculated from the IR and Raman spectra of SF_6 . Other values of the two constants could be chosen, but the values used here are representative for molecules such as PF_5 , SF_6 , IF_7 , etc. Q is a normal force constant in eq 2 but not in eq 1. The second derivative of eq 1 is dependent on the value of the exponent n and the values of the $r_{\alpha\beta}$ in the equilibrium configuration.

For MX_2 and MX_3 , both fields give the expected linear and planar triangular geometries, respectively. The bond lengths and potential energies generated by both fields are given in Tables I and II.

MX_4 . The MX_4 molecule exhibits the existence of quantum-mechanical isomers and a saddle-point geometry. The number of quantum-mechanical isomers of a given molecular geometry is a subset of the permutations on the numbering of the nuclei such that each member cannot be reached from another by a real rotation. The number of saddle-point geometries is given by the number of ways one can position the particles such that the net force on each is zero minus the number of minima. MX_4 has an equilibrium geometry with two quantum-mechanical isomers and one saddle-point geometry with three quantum-mechanical isomers. Both fields predict the equilibrium and saddle-point geometries to have T_d and D_{4h} symmetries, respectively. With field I, the Δr , $1/r$, and total energies are all lower for the T_d geometry (see Table I). Each isomer of the equilibrium T_d geometry is connected to all three isomers of the saddle-point D_{4h} geometry by a set of coordinates analogous to q_1 in Figure 1.

There is the possibility that the saddle-point geometry does not sit atop a maximum in the multidimensional curve that connects

Table II. Energies of the Equilibrium and Saddle-Point Geometries of MX_n Molecules Using the $(\theta - \pi)$ Potential

species (sym)	energy, hartrees	species (sym)	energy, hartrees
MX_3	1.1276	$\text{MX}_6 (D_{3h})$	10.2640
$\text{MX}_4 (T_d)$	3.1162	$\text{MX}_6 (C_{3v})$	10.4383
$\text{MX}_4 (D_{4h})$	3.3692	$\text{MX}_6 (D_{6h})$	11.2764
$\text{MX}_5 (D_{3h})$	6.2020	$\text{MX}_7 (C_1)$	15.2227
$\text{MX}_5 (C_{4v})$	6.2147	$\text{MX}_7 (D_{5h})$	15.2231
$\text{MX}_5 (D_{5h})$	6.7658	$\text{MX}_7 (C_{2v}[1,4,2])$	15.2248
		$\text{MX}_7 (C_{3v}[1,3,3]s)$	15.2253
		$\text{MX}_7 (C_{2v}[1,2,4])$	15.4468
		$\text{MX}_7 (C_{3v}[1,3,3]e)$	15.4509
		$\text{MX}_7 (C_{6v})$	15.7896
		$\text{MX}_7 (D_{7h})$	16.9146

one geometry with another (as shown in Figure 1) but rather sits in a shallow depression with two maxima to either side of it; i.e., there are other nonsymmetrical geometries that are also saddle-point geometries. This is easily shown not to be correct by placing the system at the symmetric saddle-point geometry (in this case the D_{4h} one), assigning a minute amount of momentum to one of the particles, and following the course of the trajectory. In this case and in all others, the system slides down the potential curve to the equilibrium configuration.

This is equivalent to a numerical determination of coordinates like q_1 of Figure 1. The method circumvents the problem of having to determine the transformation from the Cartesian basis, where the derivatives can be calculated, to the q_1 basis function where the exact functional form is unknown but value of which could be determined numerically point by point.

MX_5 . Much has been written about MX_5 molecules since Berry's paper on quantum-mechanical tunneling in PF_5 and AsF_5 .^{24,25} In addition to the equilibrium geometry (20 isomers) and the C_{4v} saddle-point geometries (30 isomers), there is another saddle-point geometry (24 isomers) with symmetry D_{3h} (see Tables I and II). The details of the structure of the C_{4v} geometry defined by fields I and II are given in Figure 2. Note that field I generates two bond lengths for both the D_{3h} and C_{4v} geometries, with the axial bonds longer than the equatorial in the former but with the single axial bond shorter in the latter. The transverse radial bond angle in the C_{4v} geometry is 152° (field I). This is an important result because it means that, in pseudorotations, the fact that the axial and equatorial pairs do not meet halfway (150°) but meet at 152° (more exactly at 151.8°) is not the result of any quantum-mechanical property of the central atom but is a result of geometry.²⁶ The barrier heights resulting from fields I and II are 2.07 and 7.96 kcal/mol, respectively.

MX_6 . This is another molecule for which a great deal has been written on the subject of its isomer interconversions.²⁷⁻³¹ Besides the equilibrium geometry (30 isomers), there are three saddle-point geometries with symmetries D_{3h} (120 isomers), C_{3v} (144 isomers), and D_{6h} (120 isomers), with the last two not chemically connected to the first two (see Tables I and II). As can be seen in Figure 1, both field I and field II elongate the D_{3h} structure axially. Counterrotation of the opposite faces of an octahedron without axial elongation gives bond angles of 90, 70.5, and 131.8° for the three angles shown in the figure. This suggests that in tris(bidentate)metal complexes, nondissociative intramolecular rearrangement might occur through a C_{2v} trigonal-prismatic intermediate, if the ligands prefer a larger bite angle (θ_{12} in Figure 1), or through a D_{3h} one, if a smaller one is preferred (θ_{14} in Figure 1). However, both bite angles are less than the original angle of

(24) Berry, R. S. *J. Chem. Phys.* **1960**, *32*, 933.(25) Berry, R. S. *Rev. Mod. Phys.* **1960**, *32*, 447.(26) Hoskin, L. C.; Lord, R. C. *J. Chem. Phys.* **1967**, *46*, 2402.(27) Ray, P.; Dutt, N. K. *J. Indian Chem. Soc.* **1943**, *20*, 81.(28) Bailar, J. C., Jr. *J. Inorg. Nucl. Chem.* **1958**, *8*, 165.(29) Springer, C. S., Jr.; Sievers, R. E. *Inorg. Chem.* **1967**, *6*, 852.(30) Brady, J. E. *Inorg. Chem.* **1969**, *8*, 1208.(31) Serpone, N.; Bickley, D. G. *Prog. Inorg. Chem.* **1972**, *17*, 391.(23) *Tables of Interatomic Distances and Configurations in Molecules and Ions* Special Publication No. 18; The Chemical Society: London, 1956; Supplement, p 1059.

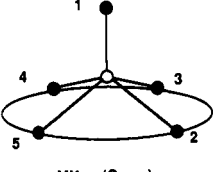
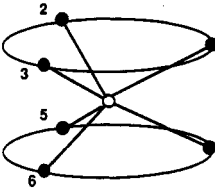
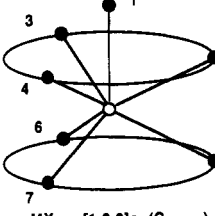
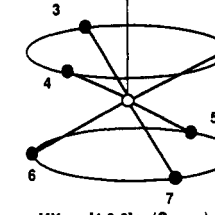
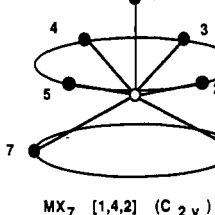
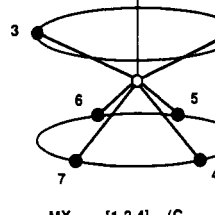
		Potential Function			
		$1/r$ (Field I)		$\theta - \pi$ (Field II)	
		i	j	θ_{ij}	θ_{ij}
	1	1	2	105.0°	105.0°
	2	2	3	87.0°	86.0°
	1	1	2	85.0°	87.0°
		1	4	77.0°	71.0°
		1	5	134.0°	132.0°
	1	1	2	69.0°	69.0°
	2	1	5	135.0°	133.0°
	5	2	3	108.0°	108.0°
		2	5	66.0°	64.0°
		2	6	126.0°	126.0°
	1	1	2	73.0°	73.0°
	2	1	5	129.0°	128.0°
	5	2	3	112.0°	112.0°
		2	5	79.0°	79.0°
		2	6	158.0°	158.0°
	1	1	2	81.0°	81.0°
	2	1	6	144.0°	144.0°
	6	2	3	96.0°	97.0°
		2	4	161.0°	162.0°
		2	5	81.0°	80.0°
		2	6	76.0°	75.0°
	1	1	2	65.0°	64.0°
	2	1	4	118.0°	116.0°
	4	2	3	130.0°	128.0°
		2	4	72.0°	74.0°
		2	6	134.0°	132.0°
		4	5	87.0°	90.0°
		4	6	124.0°	124.0°
	4	7	67.0°	64.0°	

Figure 2. Saddle-point geometries for MX_n molecules using the $1/r$ and $(\theta - \pi)$ potential functions showing the bond lengths in Å and the bond angles in degrees. For the $(\theta - \pi)$ potential function, all bond lengths are 1.56 Å.

90° in the octahedral configuration.

MX_7 . The last member of this series also has been the subject of much theoretical^{15,32-35} and experimental discussion. Besides

Table III. Energies of the Equilibrium and Saddle-Point Geometries of MX_7 Using the $1/r^n$ Potential

sym	energy, hartrees				
	$n = 1^a$	$n = 2^a$	$n = 3^a$	$n = 4^a$	$n = 4^c$
D_{5h}	5.4749	1.3118	0.3364	8.7770	0.7317
$C_{2v}[1,4,2]$	5.4767	1.3129	0.3368	8.7767	0.7326
$C_{3v}[1,3,3]s$	5.4770	1.3131	0.3369	8.7790	0.7328
$C_{2v}[1,2,4]$	5.5605	1.3732	0.3693	10.2552	
$C_{3v}[1,3,3]e$	5.5623	1.3747	0.3702	10.3055	

^a $k = 5.90$ mdyne/Å; $Q = 1.228$ mdyne Åⁿ⁺¹. ^b Same constants but energy multiplied by 100. ^c $k = 5.90$ mdyne/Å; $Q = 12.28$ mdyne Å².

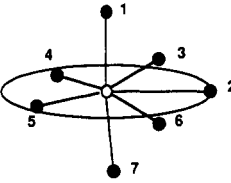
		i	j	θ_{ij}	i	j	θ_{ij}	i	j	θ_{ij}
	1	2	90.0°	2	4	143.0°	3	7	96.0°	
	1	3	84.0°	2	5	145.0°	4	5	72.0°	
	1	4	100.0°	2	6	74.0°	4	6	141.0°	
	1	5	83.0°	2	7	88.0°	4	7	82.0°	
	1	6	93.0°	3	4	72.0°	5	6	73.0°	
	1	7	178.0°	3	5	139.0°	5	7	99.0°	
	2	3	73.0°	3	6	147.0°	6	7	86.0°	

Figure 3. Lowest energy geometry of MX_7 using the $(\theta - \pi)$ potential function. Shown are the bond angles in degrees subtended at the central atom by the ij pairs; the bond lengths are all equal to the input value.

the MX_7 molecules, examples of which are IF_7 ³⁶ and ReF_7 ,³⁷ there is the question of the structure of MX_6 molecules that have a nonbonding pair of electrons in their valence shell. Examples of this type of molecule are XeF_6 ^{20,38,39} and the anions SbX_6^{3-} and TeX_6^{3-} ($X = Cl, Br, \text{ or } I$).⁴⁰ The principal question that has been raised by all these studies is whether or not the equilibrium geometry of MX_7 has D_{5h} symmetry. Since fields I and II give different equilibrium geometries, we discuss the two cases separately.

Field I. The MX_7 arrangement has besides the D_{5h} equilibrium geometry (504 isomers) six saddle-point geometries which have (in order of increasing energy) symmetries $C_{2v}[1,4,2]$ (2520 isomers), $C_{3v}[1,3,3]s$ (1680 isomers), $C_{2v}[1,2,4]$ (2520 isomers), $C_{3v}[1,3,3]e$ (1680 isomers), C_{6v} (840 isomers), and D_{7h} (720 isomers). The details of structure of these saddle-point geometries are shown in Figure 2. The first can be considered to be a trigonal prism capped on a square face, the second an octahedron capped on a face, the third a trigonal prism capped on an edge, and the fourth a trigonal prism capped on a triangular face. The fifth is simply a capped regular hexagon, and the sixth is a regular heptagon (these two are not shown in the figure). The designations in the square brackets show the clustering of particles in planes down the principal rotation axis and whether one set is staggered (s) or eclipsed (e) by another. The energies of these geometries are given in Table I. The energy separations between the equilibrium geometry and the first two saddle-point geometries are 1.129 and 1.317 kcal/mol, respectively. Even with relatively stiff force constants, an MX_7 molecule is a very dynamic system, with three easily accessible geometries.

Earlier studies using static force fields^{15,32} showed that the order of the energies of the equilibrium and saddle-point geometries is dependent on the value of n in eq 1, with a change in the order at $n = 3.5$ from D_{5h} to C_2 . The dynamic force field can be made to imitate the static by increasing the magnitude of k relative to Q . This happens automatically as the value of n is increased, and as is shown in Table III, the order of the energies of the D_{5h} and

(32) Claxton, T. A.; Benson, G. C. *Can. J. Chem.* **1966**, *44*, 157.

(33) Muetterties, E. L.; Gussenberger, L. J. *J. Am. Chem. Soc.* **1974**, *96*, 1748.
 (34) Adams, W. J.; Thompson, H. B.; Bartell, L. S. *J. Chem. Phys.* **1970**, *53*, 4040.
 (35) Bartell, L. S.; Rothman, M. J.; Gavezotti, A. *J. Chem. Phys.* **1982**, *76*, 4136.
 (36) Lord, R. C.; Lynch, M. A., Jr.; Schumb, W. C.; Slowinski, E. J., Jr. *J. Am. Chem. Soc.* **1950**, *72*, 522.
 (37) Jacob, E. J.; Bartell, L. S. *J. Chem. Phys.* **1970**, *53*, 2231, 2235.
 (38) Gavin, R. M., Jr.; Bartell, L. S. *J. Chem. Phys.* **1968**, *48*, 2460, 2466.
 (39) Pitzer, K. S.; Bernstein, L. S. *J. Chem. Phys.* **1975**, *63*, 3849.
 (40) Adams, C. J.; Downs, A. J. *J. Chem. Soc. D* **1970**, 1699.

$C_{2v}[1,4,2]$ is reversed between $n = 3$ and $n = 4$. The bond lengths are all about 1.58 Å, and the particles lie close to the sphere that they are constrained to be on in the statics calculations. If the value of Q is increased from 1.228 to 12.28, then the bond lengths are longer (about 1.7 Å) and the D_{5h} structure is again the lowest energy geometry. Thus, the dynamics results include the static.

Field II. The equilibrium geometry is now C_1 (5040 isomers) with seven saddle-point geometries (the six from above plus the equilibrium geometry from above). The equilibrium geometry is shown in Figure 3, and some of the saddle-point geometries are shown in Figure 2. The energies associated with all geometries are shown in Table II. Clearly, field II creates a fluxional nightmare. Molecules for which field II gives an accurate representation of the repulsive potential would exhibit a ground-state dipole moment.⁴¹

Conclusions

Fields I and II provide insight into the preferred geometries of MX_n molecules. Field I is a more realistic field because it allows as many different bond lengths as there are local symmetries in a given MX_n structure. Field II on the other hand generates geometries that are independent of any bond length assigned to a MX_n structure and thus provides a standard for geometry in

molecules where all pairs of the peripheral atoms try to be diametrically opposite one another. For MX_4 and MX_6 molecules, the energies of the equilibrium geometries are well below those of the nearest saddle-point ones, yet for MX_5 and MX_7 molecules, using the same force constants, there are saddle-point geometries that are easily accessible from the equilibrium geometry. These results agree with experimental results and imply that it is the repulsive interactions between the peripheral atoms and the intrinsic geometry of the molecules that determine their dynamic behavior. In addition, the details of the geometries are also in agreement with the results of quantum-mechanical calculations:^{21,35} in MX_5 , the axial bonds are longer than the equatorial ones, whereas in MX_7 they are shorter. The dynamical calculations can be made to imitate statics calculations by increasing the magnitude of the bond stretch force constant relative to the force constant Q . All isomers of a given geometry have the same potential energy with the result that derived statistical mechanical properties will have no bias.

In future work, we will use these simple potentials to study the details of isomer interconversion in MX_n molecules by scaling the force constants to give approximately correct vibrational frequencies and barrier heights.

Acknowledgment. H.-L.C. and J.F.G. acknowledge a grant from the South Carolina Energy Research and Development Center that enabled the purchase of the Digital MicroVax II computer.

(41) Kaiser, E. W.; Muentner, J. S.; Klemperer, W.; Falconer, W. E. *J. Chem. Phys.* 1970, 53, 53.

Contribution from the Fachbereich Chemie, Philipps-Universität, D-3550 Marburg, FRG, and Institute of General and Inorganic Chemistry, Bulgarian Academy of Sciences, 1040 Sofia, Bulgaria

Local and Cooperative Jahn-Teller Distortions of Ni^{2+} and Cu^{2+} in Tetrahedral Coordination

Dirk Reinen,*[†] Michail Atanasov,[‡] Georgi St. Nikolov,[‡] and Friedhelm Steffens[†]

Received July 8, 1987

A vibronic coupling model, including spin-orbit interactions, is presented and used to explain the sign and magnitude of observed Jahn-Teller distortions of Cu^{2+} and Ni^{2+} ions in tetrahedral coordination. It is demonstrated that the Jahn-Teller coupling is rather large for Cu^{2+} (2T_2 ground state) and generally dominates over steric ligand, geometric packing, or spin-orbit effects, leading to compressed tetrahedra with D_{2d} symmetry. In contrast Ni^{2+} (3T_1 ground state) undergoes much smaller Jahn-Teller interactions, and static distortions (elongated D_{2d} geometry) are not always expected. The lowering of the vibronic constants for Ni^{2+} as compared to Cu^{2+} is mainly due to the configuration interaction between the 3T_1 ground and excited states. The vibronic coupling analysis is based on spectroscopic and structural results of " CuO_4 ", " CuF_4 ", and " NiO_4 " chromophores in various host structures. A quantitative discussion of the Jahn-Teller stabilization energies for the minima in the $T \otimes (e + t_2)$ adiabatic potential surface is given. The influence of elastic interactions between the tetrahedra (cooperative Jahn-Teller effect) on the ground-state splitting and on the extent of the local Jahn-Teller distortion is also considered. An essential energy contribution to the term splittings may arise from elastic interactions of this kind in structures with widely interconnected polyhedra.

Introduction

Cu^{2+} and Ni^{2+} ions in tetrahedral coordination have orbitally degenerate ground states 2T_2 and 3T_1 , respectively and are expected to be subject to Jahn-Teller forces.¹ The induced symmetry lowering and term splittings due to the minima of the adiabatic Jahn-Teller (JT) surface can be detected by spectroscopic and structural studies. Whether a static or dynamic Jahn-Teller effect prevails depends on the depth of the various minima of the adiabatic potential surface (APS). While stable minima are known to arise only from second-order contributions for Cu^{2+} in octahedral coordination, in tetrahedral geometry such points are already produced by first-order terms. Static Jahn-Teller distortions have been observed in the case of $CuCl_4^{2-}$ entities and are interpreted within the angular overlap model (AOM).² Unlike Cu^{2+}

the structural and spectral data on tetrahedral Ni^{2+} are scarce because this ion only reluctantly adopts this coordination.³ The incorporation of Cu^{2+} and also Ni^{2+} into the tetrahedral sites of the spinel structure is possible, however, if the octahedral sites are blocked by Cr^{3+} .³

The aim of the present paper is to explain the sign and the magnitude of the static Jahn-Teller distortions in spinels with the constitution $[M_xZn_{1-x}]^{II}[Cr_2]^{III}O_4$ ($M = Cu^{2+}, Ni^{2+}$; o = octahedral; t = tetrahedral) on the basis of spectral and structural data. We will first present a vibronic coupling model—including spin-orbit coupling—which allows us to describe the Jahn-Teller distortions of tetrahedral Cu^{2+} and Ni^{2+} complexes. Then we will analyze spectral and structural data of MO_4 chromophores ($M = Ni^{2+}$,

[†] Philipps-Universität.

[‡] Bulgarian Academy of Sciences.

(1) Reinen, D. *Comments Inorg. Chem.* 1983, 2, 227.

(2) Bacci, M. *J. Phys. Chem. Solids* 1980, 41, 1267.

(3) Reinen, D.; Allmann, R.; Baum, G.; Jakob, B.; Kaschuba, U.; Massa, W.; Miller, G. *J. Z. Anorg. Allg. Chem.* 1987, 548, 7.